

Resonance Curves of Multidimensional Chaotic Systems

Glenn Foster, Alfred W. Hübler and Karin Dahmen

Abstract We study resonance curves of nonlinear dynamical systems with chaotic forcing functions. We use the calculus of variations to determine the forcing function that induces the largest response. We compute the resonant forcing for a set of model systems and determine the response of the dynamical system to each forcing function. We show that the response is largest if the model system matches the dynamical system. We find that the signal to noise ratio is particularly large if one of the Lyapunov exponents is large.

1 Introduction

The limiting response of damped nonlinear oscillators to sinusoidal forcing functions can usually be characterized with frequency response curves and Arnold tongues. The response is typically largest and synchronized, *-i.e.* the periodic forcing function is in resonance, if the driving frequency is within a frequency interval centered around the frequency of the unperturbed oscillator. Therefore the frequency response curve is often called a resonance curve. Resonance curves can be derived with secular perturbation theory and have a large range of important applications, including synchronization [1], stochastic resonance [2, 3], and nonlinear transport phenomena [4]. Probably the most important application is resonance spectroscopy,

Glenn Foster
Department of Physics, University of Illinois at Urbana-Champaign, Urbana, Illinois 61801, e-mail: gfoster@uiuc.edu

Alfred W. Hübler
Department of Physics, University of Illinois at Urbana-Champaign, Urbana, Illinois 61801 e-mail: a-hubler@uiuc.edu

Karin Dahmen
Department of Physics, University of Illinois at Urbana-Champaign, Urbana, Illinois 61801 e-mail: dahmen@uiuc.edu

-i.e. the identification of dynamical systems based on peaks in resonance curves. However only undamped and weakly damped linear oscillators, have sharp resonance peaks, whereas the quality of the resonance peak is small for systems with large damping or large nonlinearity [5, 6]. In 1987 Reiser et al. [7] showed that forcing functions which are proportional to the time reflected unperturbed dynamics has zero reaction power and produces a large response even for damped oscillators with a large nonlinearity. And in the same year Kautz [8] used optimal control theory [9] to derive minimal energy forcing functions to determine the most problem escape paths and activation energies of damped nonlinear oscillators. Beale [10] and Grassberger [11] generalized Kautz's approach to systems which do not necessarily have an energy function. Grassberger shows that the initial exponential growth rate of optimal forcing functions is equal and opposite to the negative Lyapunov exponent, if there is only one negative Lyapunov exponent. Chang et al. [12] use minimal escape paths of damped nonlinear oscillators to compute resonance curves. Plapp et al. [13] show that the minimization of the energy and the minimization of the reaction power lead to similar solutions, Krempl et al [14] apply the methodology to quantum systems, and later Wargitsch et al. [15] show that the solutions are the same if the duration of the pulse is optimized. Graham et al. [16] introduce generalized potentials for dynamical systems and Beri et al. [17] simplify the boundary problem associated with Grassberger's equations with topological methods and solve it numerically. Only recently Foster et al. [18] published analytical solutions to the boundary value problem for systems with multiple or no negative Lyapunov exponents and show that the scalar product of the optimal forcing function and the separation of nearby trajectories is a conserved quantity.

In this paper, we use the analytical solution by Foster et al. to determine resonance curves of chaotic systems for system identification. We show that minimal escape path resonance curves have a large signal-to-noise ratio. We consider a dynamical systems, and a set of models where one of these models has the same mapping function as the dynamical system. Typically, the set of models is parameterized with a model parameter a_m . For each model we determine optimal forcing functions, apply the optimal forcing function to the dynamical system, and determine the response. The response versus the model parameter is called the resonance curve. This is a generalization of the traditional meaning of resonance curves. For instance, if the dynamical system is a weakly damped, linear oscillator, and the models are set weakly damped of linear oscillators where the frequency is the model parameter, then resonant forcing functions are sine-functions with a time dependent amplitude and the resonance curve is very similar to a standard frequency response curve.

2 Resonant Forcing and Resonance Curves

We consider the iterated map dynamics where the mapping function f contains an unknown parameter a :

$$\mathbf{x}_{n+1} = \mathbf{f}(\mathbf{x}_n, a) + \mathbf{F}_n + \mathbf{r}_n \quad (1)$$

where $\mathbf{x}_n \in R^d$ denotes the state of the d -dimensional system at time step $n = 0, 1, \dots, N-1$, and f is differentiable in \mathbf{x} within a given region of interest. $\mathbf{F}_n \in R^d$ is a small forcing function at time step n . $\mathbf{r}_n = (r_{n,1}, r_{n,2}, \dots, r_{n,d})$ is very small, additive, band-limited, white noise where each component at each time step is a random number with variance $\langle (r_{n,i})^2 \rangle = r^2/(Nd)$ without correlations, i.e. $\langle r_{n,i}r_{n,j} \rangle = 0$ for $i \neq j$ where $i, j = 1, 2, \dots, d$. The response is predicted with a model:

$$\mathbf{X}_{n+1} = \mathbf{f}(\mathbf{X}_n, a_m) + \mathbf{F}_n \quad (2)$$

where \mathbf{X}_n is the state of the model system at time n . The model parameter a_m is within a given range $a_{min} \leq a_m \leq a_{max}$ which is assumed to contain the correct value, i.e. $a_{min} \leq a \leq a_{max}$. If the model is exact ($a = a_m$, $\mathbf{x}_0 = \mathbf{X}_0$, $\mathbf{r}_n = 0$), the difference between the observed response, $R^2(\mathbf{F}) = |\mathbf{x}_N - \mathbf{y}_N|^2$, and the predicted response $R_m^2 = |\mathbf{X}_N(a_m) - \mathbf{Y}_N(a_m)|^2$ is zero, where y_n is the unperturbed system dynamics, Y_n is the unperturbed model dynamics, and $\mathbf{F} = \{\mathbf{F}_0, \mathbf{F}_1, \dots, \mathbf{F}_{N-1}\}$ is a forcing function. The fact that $D^2(\mathbf{F}, a_m) = R^2 - R_m^2$ is zero if the model is correct, can be used for system identification. System identification is unique if $D^2(\mathbf{F}, a_m)$ has only one root. The number of roots depends on the forcing function and the noise. In order to achieve a large signal to noise ratio we study the final response of the system to a set of forcing functions, which contains the resonant forcing function. The resonant forcing function is the forcing function which produces the largest response among all forcing functions with the same magnitude $F^2 = \sum_{n=0}^{N-1} |\mathbf{F}_n|^2$. In the case of a laser field F^2 is a measure for the total energy of the radiation pulse [19, 20]. F is a metric for the forcing function \mathbf{F} . We consider a set of forcing functions S , where all forcing functions have the same magnitude F , and each forcing function maximizes the final response of a particular model with model parameter a_m . Then the forcing function depends on the model parameter $\mathbf{F} = \mathbf{F}(a_m)$. If the model is correct the forcing function maximizes the response of the dynamical system among all forcing functions with the same magnitude. Consequently $\mathbf{F}(a)$ maximizes the response of the system among all forcing functions within the set S . The function $R(\mathbf{F}(a_m))$ is called a resonance curve. The resonance curve has an absolute maximum for $a_m = a$, i.e. $R(\mathbf{F}(a)) \geq R(\mathbf{F}(a_m))$ for all a_m in the range $a_{min} \leq a_m \leq a_{max}$.

We use the calculus of variations with Lagrange function

$$L = R_m^2/2 + \sum_{n=0}^{N-1} \mathbf{k}_n (\mathbf{x}_{n+1} - \mathbf{f}(\mathbf{x}_n) - \mathbf{F}_n) + \mu (\mathbf{F}_n)^2/2 \quad (3)$$

to determine the forcing function with yields the largest final response R_m^2 where $\mathbf{Y}_0 = \mathbf{X}_0$, $\mathbf{k}^{(n)}$ and μ are Lagrange multipliers. The stationary points of the Lagrange function provide necessary conditions for the maximum response. Elimination of the Lagrange multipliers $\mathbf{k}^{(n)}$ gives the following set of equations for the resonant forcing function

$$(J_{n+1}(b))^T \mathbf{F}_{n+1} = \mathbf{F}_n \quad (4)$$

and

$$\mathbf{x}_N - \mathbf{y}_N = -\mu \mathbf{F}_{N-1} \quad (5)$$

where $n=0,1,\dots,N-1$, and $J_n(b) = (\partial f_i(b)/\partial X_j)|_{\mathbf{x}_n}$ is the Jacobi matrix evaluated at \mathbf{X}_n . The dynamics of a small displacement $\mathbf{d}_n = \mathbf{X}_n - \tilde{\mathbf{X}}_n$ between two neighboring trajectories at \mathbf{X}_n and $\tilde{\mathbf{X}}_n$ is $\mathbf{d}^{(n+1)} = J^{(n)}\mathbf{d}^{(n)}$. Hence the scalar product of the resonant forcing and the displacement is a conserved quantity

$$P = \mathbf{F}_n \cdot \mathbf{d}_{n+1} \quad (6)$$

for $n = 0, 1, \dots, N - 1$. We used no approximations to derive Eq.(6). The resonant forcing function complements the displacement dynamics of the model. If the system is one-dimensional, then the resonant forcing is proportional to the inverse of the displacement at each time step, i.e. $F_n = P/d_{n+1}$. Thus if the displacement dynamics is periodic, then the resonant forcing has the same periodicity and if the displacement dynamics is chaotic, then the resonant forcing has the same type of aperiodicity. Figure 1 shows that the displacement and the optimal forcing function are complementary for a chaotic logistic map dynamics, $x_{n+1} = ax_n(1 - x_n) + F_n$, where $a = 3.61$, $N = 15$, $F = 0.0001$ and $x_0 = 0.897$.

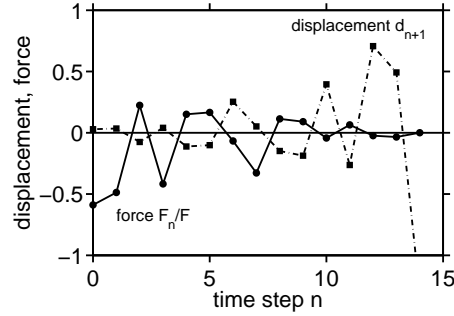


Fig. 1 The resonant forcing F_n (circles) and the displacement of two neighboring trajectories d_{n+1} (squares) versus time step n for a chaotic logistic map dynamics. This plot illustrates that the resonant forcing complements the displacement of neighboring trajectories of the unperturbed system, i.e. $F_n d_{n+1} = \text{constant}$. When the magnitude of the displacement is large, then the magnitude of the resonant force is small, and if the displacement is positive, the resonant force is negative.

3 Resonance Curves for Small Forcing Functions

Next we assume that the forcing function is small and expand the Jacobi matrix about the unperturbed dynamics to lowest order, i.e. $J_n \approx (\partial f_i/\partial x_j)|_{\mathbf{y}_n}$. To lowest order, the difference between the trajectory of the driven system and the unperturbed system reads: $\mathbf{x}_N - \mathbf{y}_N = \mathbf{F}_{N-1} + \sum_{n=1}^{N-1} (\prod_{i=1}^n J_{N-i}) \mathbf{F}_{N-1-n}$. With Eq. (4) and Eq. (5) we obtain

$$M\mathbf{F}_{N-1} = -\mu\mathbf{F}_{N-1} \quad (7)$$

where $M = I + \sum_{n=1}^{N-1} M_n$ and $M_n = (\prod_{i=1}^n J_{N-i}) (\prod_{i=1}^n J_{N-i})^T$. I is the identity matrix. M is a symmetric matrix with up to d orthogonal eigenvectors \mathbf{e}_i , where $M\mathbf{e}_i = \mu_i\mathbf{e}_i$, $i = 1, 2, \dots, d$ and $\mathbf{e}_i^T = 1$. The corresponding eigenvalues μ_i are positive. The eigenvectors of matrix M are the solutions of Eq. (7) $\mathbf{F}_{N-1} = \pm F_{N-1}\mathbf{e}_i$, where $F_{N-1} = |\mathbf{F}_{N-1}|$ and $\mu = -\mu_i$. Eq. (4) and Eq. (7) yield $F^2 = \mu_i F_{N-1}^2$ and $R^2 = (\mathbf{x}_N - \mathbf{y}_N)^2 = \mu_i^2 (F_{N-1})^2 = \mu_i F^2$. Hence the final forcing which parallels the eigenvector with the largest eigenvalue of M , $\hat{\mu} = \max\{\mu_i\}$ produces the largest response, and the largest response is

$$R^2 = \hat{\mu}F^2 \quad (8)$$

and with Eq. (7) we obtain

$$\hat{\mathbf{F}}_{N-1} = \pm \frac{F}{\sqrt{\hat{\mu}}}\hat{\mathbf{e}} \quad (9)$$

where $\hat{\mathbf{e}}$ is the eigenvector that corresponds to the largest eigenvalue of M , and for $n = 0, 1, \dots, N-2$ the time dependence of the resonant forcing function is $\mathbf{F}_n = \pm \frac{F}{\sqrt{\hat{\mu}}} \left(\prod_{i=1}^{N-1-n} (J_{n+i})^T \right) \hat{\mathbf{e}}$. Figure 2 shows resonance curves of a chaotic Henon

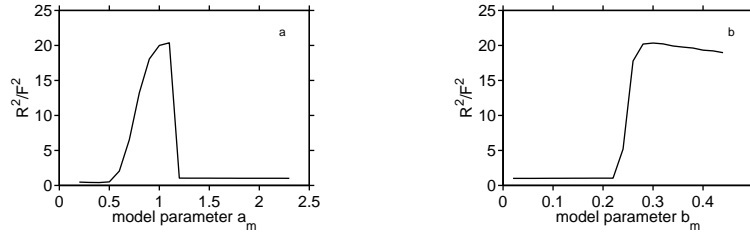


Fig. 2 The resonance curve of a chaotic Henon map versus model parameter a_m , where $b_m = b$ (a) and versus model parameter b_m where $a_m = a$. The parameters are $a = 1.08$, $b = 0.3$, $N = 3$ and $F = 0.0001$.

map dynamics as a function of the map parameter a_m and b_m . The Henon map is $x_{1,n+1} = 1 - a(x_{1,n})^2 + x_{2,n} + F_{1,n}$ and $x_{2,n+1} = bx_{1,n} + F_{2,n}$, where $\mathbf{x}_n = (x_{1,n}, x_{2,n})$ is the state and $\mathbf{F}_n = (F_{1,n}, F_{2,n})$ is the forcing function. a and b are parameters. The magnitude of the forcing function is $F = 0.0001$, the noise level is $r = 0$, and the number of time steps is $N = 3$. The numerical values of the peak location of the resonance curve is in good agreement with the system parameters $a = 1.08$, $b = 0.3$.

For systems with only one variable $x_{n+1} = f(x_n, a) + F_n + r_n$, the eigenvalue of M is (see Eq. (7))

$$\hat{\mu} = 1 + \sum_{n=1}^{N-2} \prod_{i=1}^n \left(\frac{\partial f}{\partial x} \Big|_{y^{(N-i)}} \right)^2 \quad (10)$$

From Eq. (4) we obtain for the resonant forcing function

$$F^{(n)} = \prod_{i=1}^{N-n-1} \frac{\partial f}{\partial x} \Big|_{y^{(n+i)}} F^{(N-1)} \quad (11)$$

where $F^{(N-1)} = \pm F / \sqrt{\hat{\mu}}$. The response to the resonant forcing function is $R =$

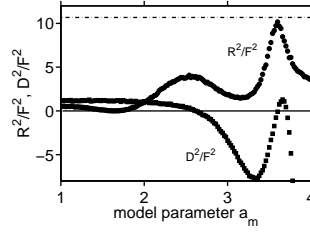


Fig. 3 The resonance curve for a chaotic logistic map (circles) and deviation D between the response model and the response of the dynamical system for a set of sinusoidal forcing functions (squares) versus the model parameter a_m . The number of time steps is $N = 4$, the noise level is $r = 0.0005$, and the magnitude of the forcing function is $F = 0.001$. The dashed line indicates the theoretical result for the maximum of the resonance curve given by Eq. (8). The maximum of the resonance curve, as well as one of the three roots of D are close to the parameter value of the dynamical system, $a = 3.6$.

$\sqrt{\hat{\mu}}F$. Fig. 3 shows the resonant forcing function (Eq. (11)) and the displacement dynamics for a chaotic logistic map dynamics $x^{(n+1)} = 3.61x^{(n)}(1 - x^{(n)}) + F^{(n)}$, for $n = 0, 1, \dots, 14$, with the initial condition $y^{(0)} = x^{(0)} = 0.34$. The magnitude of the forcing function $F = 0.0001$. With Eq. (10) we compute $\hat{\mu} = 1500$. We find that the predicted response $R = 0.00387$ is close to the numerical value $R = 0.00378$.

The matrix $M^{(N)}$ describes how the magnitude of a displacement grows $|\mathbf{d}^{(N)}|^2 = (\mathbf{d}^{(0)})^T M^{(N)} \mathbf{d}^{(0)}$. If $\mu_i^{(n)}$ are the eigenvalues of $M^{(n)}$ then the Lyapunov exponents are the limits $\lambda_i = \lim_{n \rightarrow \infty} \frac{1}{2n} \ln \mu_i^{(n)}$. The set of Lyapunov exponents will be the same for almost all starting points on an ergodic attractor.

For some chaotic systems the matrices $M^{(n)}$ have approximately the same eigenvectors and eigenvalues. For instance if the Jacobian is constant, i.e. $J^{(n)} = J^{(0)}$ for $n = 1, 2, \dots, N-1$, then $M^{(n)} = (J^{(0)})^n ((J^{(0)})^T)^n = (J^{(0)}(J^{(0)})^T)^n = (M^{(1)})^n$ since $J^{(0)}(J^{(0)})^T = (J^{(0)})^T J^{(0)}$. This is the case for coupled Bernoulli map dynamics (see Eq. (15)). If the matrices $M^{(n)}$ have approximately the same eigenvectors and eigenvalues, then the eigenvalues obey the following relation $\mu_i^{(n)} \approx (\mu_i^{(1)})^n \approx e^{2n\lambda_i}$.

If an initial displacement is parallel to the eigenvector of M that corresponds to the largest Lyapunov exponent $\hat{\lambda} = \max\{\lambda_i, i = 1, 2, \dots, d\}$, then it has the largest growth rate, i.e. $d^{(n)} = e^{n\hat{\lambda}}d^{(0)}$. The final value of the optimal forcing function $\mathbf{F}^{(N-1)}$ is parallel to the eigenvector of M that corresponds to the largest Lyapunov exponent and earlier values obey the dynamics:

$$|\mathbf{F}^{(n)}|^2 = \left(\mathbf{F}^{(N-1)}\right)^T M^{(N-n)} \mathbf{F}^{(N-1)} = \mu_i^{(N-n)} (F^{(N-1)})^2 = \frac{1}{\mu_i^n} (F^{(0)})^2 \quad (12)$$

Hence the the growth rate of the magnitude of the optimal forcing function is equal to the opposite of the largest Lyapunov exponent:

$$F^{(n)} \approx e^{-\hat{\lambda}n} F^{(0)} \quad (13)$$

Since $M = I + \sum_{n=1}^{N-1} M^{(n)}$ we estimate $\hat{\mu} \approx \sum_{n=0}^{N-1} \hat{\mu}_1^n = \frac{1-\hat{\mu}_1^N}{1-\hat{\mu}_1} \approx \frac{1-e^{2\hat{\lambda}N}}{1-e^{2\hat{\lambda}}}$. Then the response can be approximated by

$$R^2 \approx \frac{1 - e^{2\hat{\lambda}N}}{1 - e^{2\hat{\lambda}}} F^2 \quad (14)$$

An example for a mapping function with a constant Jaccobian is a system of two coupled Bernoulli maps:

$$\begin{pmatrix} x_{1,n+1} \\ x_{2,n+1} \end{pmatrix} = \begin{pmatrix} \text{mod}(ax_{1,n} + kx_{2,n} + F_{1,n}) \\ \text{mod}(bx_{2,n} + kx_{1,n} + F_{2,n}) \end{pmatrix} \quad (15)$$

where the function $\text{mod}(x) = x - [x]$ returns the decimal part of x . a and b are the growth rates and k is the coupling constant. We assume that $a > b \geq 0$. For the corresponding model dynamics with the parameters a_m , b_m , and k_m , the eigenvalues of M_1 are $\hat{\mu}_1(a_m, b_m, k_m) = 0.5(a_m^2 + b_m^2 + 2k_m^2 + (a_m + b_m)\sqrt{(a_m - b_m)^2 + 4k_m^2})$ and the eigenvectors

$$\mathbf{e} = \frac{(a_m - b_m + \sqrt{(a_m - b_m)^2 + 4k_m^2}, 2k_m)}{\sqrt{((a_m - b_m \pm \sqrt{(a_m - b_m)^2 + 4k_m^2})^2 + 4k_m^2)}} \quad (16)$$

Since the Jacobian $J_n(a_m, b_m, k_m)$ is symmetric and constant, the eigenvectors of the M_1 are eigenvectors of M_n , and the Lyapunov exponents are $\lambda_{1/2} = \frac{1}{2} \ln \mu_{1/2}^{(1)}$ and the largest Lyapunov exponent is $\hat{\lambda} = \frac{1}{2} \ln(\hat{\mu})$. If $\hat{\mu}(a, b, k) > 1$ the unperturbed dynamics is chaotic. Hence $\mathbf{F}^{(n)} = \pm (J)^{N-1-n} \frac{F}{\sqrt{\hat{\mu}}} \hat{\mathbf{e}}$. The peak value of the resonance curve is given by Eq. (17).

If $k = 0$ then $\hat{\mu}_J = a_1$, $\hat{\mu} = \frac{a_1^{2N-1}}{a_1^2-1}$, $\hat{\mathbf{e}} = (1, 0)$, $\mathbf{F}^{(n)} = \pm (a_1^{N-n-1} F / \sqrt{\hat{\mu}}, 0) = (F^{(0)} / a_1^n, 0)$, where $F^{(0)} = \pm a_1^{N-1} F / \sqrt{\hat{\mu}}$ and

$$R^2 = F^2 \frac{(a^N a_m^N - 1)^2 (a_m^2 - 1)}{(a_m^{2N} - 1)(aa_m - 1)^2} \quad (17)$$

The resonance curve does not depend on b_m . Hence the resonance curve can not be used to determine the parameter of the less chaotic dynamics b_m . For $k = 0$ the systems contains two decoupled Bernoulli maps, where $\lambda_i = \ln |a_i|$, $i = 1, 2$ is the Lyapunov exponent of each map. The resonant forcing function is in the direction of the map with the larger Lyapunov exponent. Hence if both maps have a positive Lyapunov exponent and therefore both are chaotic, then the resonant forcing function forces only the map which is more chaotic. There is no forcing of the less chaotic map. For a periodic forcing $F_{1,n} = (-1)^n F / \sqrt{N}$ and $F_{2,n} = 0$ the difference between the system response R^2 and the model response R_m^2 is

$$D^2 = \left(\left(\frac{1 - (-a)^N}{a + 1} \right)^2 - \left(\frac{1 - (-a_m)^N}{a_m + 1} \right)^2 \right) \frac{F^2}{N} \quad (18)$$

Figure 4 shows the numerical and theoretical resonance curve for a Bernoulli map dynamics and the deviation D^2 . The response to the sinusoidal forcing function and D are much smaller than the response to the optimal forcing function. Finally we

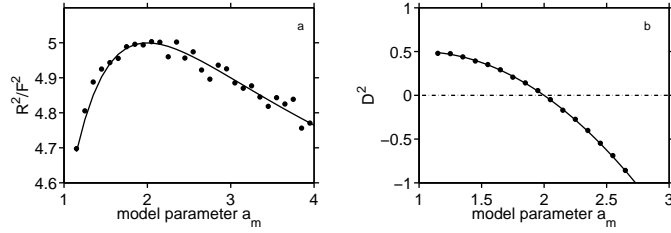


Fig. 4 The resonance curve(a) and the difference between the model response and the system response versus the model parameter (b) for a chaotic Bernoulli map with parameter $a = 2$. The continuous lines are the theoretical values given by Eq. (18) and Eq. (19). The resonance curve has an absolute maximum if the model parameter matches the system parameter. In contrast, the difference of the response is zero if the model parameter matches the system parameter.

compute the response to random forcing $\mathbf{r}_n = (r_{1,n}, r_{2,n}, \dots, r_{d,n})$ where each component of the forcing function at each time step is a random number with variance $\langle (r_{i,n})^2 \rangle = F^2 / (Nd)$ and without correlations $\langle r_{i,n} r_{j,n} \rangle = 0$ for $i \neq j$. Then the expectation value of the response is

$$R_r^2 = \left(\frac{1}{d} \sum_{i=1}^d \frac{1 - e^{2\lambda_i N}}{1 - e^{2\lambda_i}} \right) \frac{r^2}{N} \quad (19)$$

From Eq. (14) and Eq. (19) we conclude that the response for the optimal forcing is large compared to response from random forcing, if the largest Lyapunov exponent

is much larger than the other Lyapunov exponents. Fig. 5 shows the signal-to-noise ratio, i.e. the ratio response for optimal forcing and random forcing, R^2/R_r^2 , as a function of the largest Lyapunov exponent for a chaotic Bernoulli map dynamics. The signal-to-noise ratio is particularly large, if the largest Lyapunov exponent is much larger than the other Lyapunov exponents.

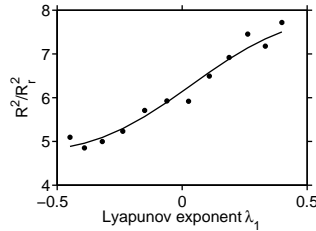


Fig. 5 Signal-to-noise ratio R^2/r_r^2 versus the largest Lyapunov exponent of a coupled Bernoulli map, where $N = 4$, $a_2 = 0.5$, $k = .2$, and $F = r = 0.0001$. The continuous line is the theoretical value given by Eq. (14) and Eq. (19). The bullets are the expectation values determined from 1000 simulations. This figure illustrates that the signal to noise ratio is particularly large if one Lyapunov exponent is significantly larger than the others.

4 Summary

We compute resonance curves of nonlinear dynamical systems with chaotic forcing functions (see Fig. 2, Fig. 3, and Fig. 4). We use the calculus of variations to determine the forcing function that induces the largest response (Eq. (4) and Eq. (5)). We find that the product of resonant forcing and the displacement of nearby trajectories is a conserved quantity (Eq. (6)), i.e. when the displacement dynamics is irregular, the resonant forcing function is irregular too (see Fig. 1). Figure 2 illustrates that the response is largest if the model system matches the dynamical system. Figure 5 shows that the signal to noise ratio is particularly large if one of the Lyapunov exponents is large. Traditional resonance curves show the limiting response to very long sinusoidal perturbations. However in many experimental situations forcing functions have to be rather short, because experimental constraints, such as the coherence length and the energy content, impose limits on the duration of a laser pulse. In this paper, resonance curves show the final response to short, but most efficient forcing functions. For damped linear oscillators, these forcing functions are sine-functions where the amplitude grows exponentially at a rate which is equal and opposite to its negative Lyapunov exponent. For quasi-periodic systems, optimal forcing functions are quasi-periodic and have a constant amplitude[21]. For chaotic one dimensional map dynamics the optimal forcing function is aperiodic

and its amplitude decreases exponentially at a rate which is equal and to its positive Lyapunov exponent. For some systems the Lyapunov exponent does not describe the evolution of small perturbation [22]. Even in this case we can conclude that for one-dimensional mapping functions, the magnitude optimal forcing function decreases on average if the magnitude of the separation of nearby trajectories increases on average and vice versa, since the product of the optimal forcing function and the separation of nearby trajectories is a conserved quantity (see Eq. 6).

Acknowledgements This material is based upon work supported by the National Science Foundation Grant No. NSF PHY 01-40179 and NSF DMS 03-25939 ITR. A.H. thanks the Santa Fe Institute for support.

References

1. I. Siddiqi, R. Vijay, F. Pierre, C. M. Wilson, L. Frunzio, M. Metcalfe, C. Rigettiand, R. J. Schoelkopf, M. H. Devoret, D. Vion, et al., *Phys. Rev. Lett.* **94**, 027005 (2005)
2. R. L. Badzey and P. Mohanty, *Nature* **437**, 962 (2005)
3. C. Wargitsch and A. W. Hubler, *Il Nuovo Ciminto* **17D**, 969 (1990)
4. S. Wimberger, R. Mannella, O. Morsch, and E. Arimondo, *Phys Rev Lett.* **94**, 130404 (2005)
5. T. Eisenhammer, A. W. Hubler, T. Geisel, and E. Luscher, *Phys.Rev. A* **41**, 3332 (1990)
6. L. E. Arsenault and A. W. Hubler, *Phys. Rev. E* **51**, 3561 (1995)
7. G. Reiser, A. W. Hubler, and E. Luscher, *Z. Naturforschung* **42a**, 803 (1987)
8. R. L. Kautz, *Phys. Lett. A* **125**, 315 (1987)
9. W. H. Fleming, *Appl. Math. Optim.* **4**, 329 (1977)
10. P. D. Beale, *Phys. Rev. A* **40**, 3998 (1989)
11. P. Grassberger, *J. Phys. A: Math. Gen.* **22**, 3283 (1989)
12. K. Chang, A. Kodogeorgiou, A. W. Hubler, and E. A. Jackson, *Physica D* **51**, 99 (1991)
13. B. B. Plapp and A. W. Hubler, *Phys. Rev. Lett.* **65**, 2302 (1990)
14. S. Krempf, T. Eisenhammer, A. Hubler, G. Mayer-Kress, and P. W. Milonni, *Phys. Rev. Lett.* **69**, 430 (1992)
15. C. Wargitsch and A. Hubler, *Phys. Rev. E* **51**, 1508 (1995)
16. R. Graham, A. Hamm, and T. Tel, *Phys. Rev. Lett* **66**, 3089 (1991)
17. S. Beri, R. Mannella, D. G. Luchinsky, A. N. Silchenko, and P. V. E. McClintock, *Phys. Rev. E* **72**, 036131 (2005)
18. G. Foster, A. W. Hubler, and K. Dahmen, *Phys. Rev. E* **75**, 0036212 (2007)
19. V. N. Smelyanskiy and M. I. Dykman, *Phys. Rev. E* **55**, 2516 (1997)
20. I. A. Khovanov, D. G. Luchinsky, R. Mannella, and P. V. E. McClintock, *Phys. Rev. Lett* **85**, 2100 (2000)
21. J. Xu and A. W. Hubler, *Phys. Rev. B* **67**, 184202 (2003)
22. G. Paladin, M. Serva, and A. Vulpiani, *Phys. Rev. Lett.* **74**, 66 (1995)